Original Article

MOLECULAR METABOLISM

PACAP attenuates hepatic lipid accumulation through the FAIM/AMPK/IRβ axis during overnutrition

Wei Luo, Jiaxin Dai, Jianmin Liu, Yongmei Huang, Ziqiong Zheng, Pei Xu, Yi Ma*

ABSTRACT

Objective: Pituitary adenylate cyclase-activating polypeptide (PACAP) was reported to attenuate hepatic lipid accumulation in overnutrition-related metabolic disorder, mediated by up-regulation of fas apoptosis inhibitory molecule (FAIM). However, how PACAP regulates FAIM in metabolic tissues remains to be addressed. Here we investigated the underlying mechanism on the role of PACAP in ameliorating metabolic disorder and examined the potential therapeutic effects of PACAP in preventing the progression of metabolic associated fatty liver disease (MAFLD).

Methods: Mouse models with MAFLD induced by high-fat diet were employed. Different doses of PACAP were intraperitoneally administrated. Western blot, luciferase assay, lentiviral-mediated gene manipulations and animal metabolic phenotyping analysis were performed to explore the signaling pathway involved in PACAP function.

Results: PACAP ameliorated the excessive hepatic lipid accumulation and inhibited lipogenesis in HFD-fed C57BL/6J mice. Mechanistically, PACAP activated the FAIM-AMPK-IRβ axis to inhibit the expression of lipid synthesis genes, and FAIM mediated the effects of PACAP. FAIM suppression via lentiviral-mediated shRNA inhibited the activation of AMPK, whereas FAIM overexpression promoted AMPK activation. PACAP increased the promoter activity of FAIM gene through activating PKA-CREB signaling pathway.

Conclusion: Our work demonstrated that the administration of PACAP represented a feasible approach for treating hepatic lipid accumulation in MAFLD. The findings reveal the molecular mechanism that PACAP increase FAIM expression and activates the FAIM/AMPK/IRβ signaling axis, thus inhibits lipogenesis to mediate its beneficial effects.

Keywords AMPK; FAIM; IRβ; PACAP; Hepatic lipid accumulation; Lipogenesis

1. INTRODUCTION

Metabolic associated fatty liver disease (MAFLD) is characterized by an excessive accumulation of triglycerides in hepatocytes [1]. There is estimated that 20–30% of the global population has been diagnosed with MAFLD and the trend is on the rise [2]. Due to its close association with obesity and type 2 diabetes mellitus (T2DM), MAFLD increases the risks for metabolic disorders, posing serious threats to public health. New insights into the pathogenesis of the overnutrition-induced fatty liver disease are of key interest.

Hepatic steatosis develops due to an imbalance of lipid homeostasis. Aberrant lipid accumulation in the liver is resulted from increased lipogenesis, decreased fatty acid β oxidation and lipoprotein efflux [3]. The accumulation of lipids in the liver activates lipid synthesis-related gene expression and causes a vicious cycle of lipid toxicity. These may progressively develop hepatocyte dysfunction, and ultimately lead to cirrhosis or hepatocellular carcinoma (HCC) [4]. *De novo* lipogenesis (DNL) is a key step in liver regulation of lipid metabolism balance. The increased hepatic DNL is a primary metabolic disorder in the pathogenesis of MAFLD [5]. Indeed, several clinical studies have shown a significantly increased incidence of DNL in obese patients compared with non-obese patients, and approximately 20–30% of lipid accumulation in the liver of obese MAFLD patients has been shown to associated with DNL [5–7]. Therefore, effective reduction of lipogenesis could be a beneficial approach to the treatment of MAFLD. Certain medications have been developed such as pioglitazone and metformin, however, limited beneficial effects have been shown on MAFLD. Currently, there are no approved drugs available specifically for the management of MAFLD, and there is growing interest in therapeutic strategies.

Pituitary adenylate cyclase activating peptide 38 (PACAP38, or PACAP) is a conserved pleiotropic neuropeptide belonging to the glucagon superfamily [8]. PACAP activates the cAMP/PKA signaling pathway and participates in various physiological functions such as cell proliferation and energy homeostasis [9]. It has been reported that serum triglycerides and cholesterol in PACAP knockout mice were significantly higher than in littermates. PACAP null mice developed microvascular fat accumulation in the liver, skeletal muscle, and heart [10], and

Department of Cellular Biology, Institute of Biomedicine, National Engineering Research Center of Genetic Medicine, Key Laboratory of Bioengineering Medicine of Guangdong Province, Jinan University, 601 Huangpu Ave. West, Guangzhou 510632, Guangdong Province, China

*Corresponding author. E-mail: tmayi@jnu.edu.cn (Y. Ma).

Received May 23, 2022 • Revision received July 23, 2022 • Accepted August 25, 2022 • Available online 30 August 2022

https://doi.org/10.1016/j.molmet.2022.101584

Abbreviations

AMPK	AMP-activated protein kinase
cAMP	cyclic adenosine monophosphate
CD	chow diet
CREB	cAMP responsive element binding protein
DNL	*de novo* lipogenesis
FAIM	fas apoptosis inhibitory molecule
FAS	fatty acid synthase
HDL-c	high density lipoprotein cholesterol
H&E	hematoxylin and eosin
HFD	high-fat diet
HMGCR	3-hydroxy-3-methylglutaryl-CoA reductase
IPGTT	intraperitoneal glucose tolerance test
IPITT	intraperitoneal insulin tolerance test
LDL-c	low density lipoprotein cholesterol
IRβ	insulin receptor β
MAFLD	metabolic associated fatty liver disease
PA	palmitic acid
PAC1	PACAP type I receptor
PACAP	pituitary adenylate cyclase activating polypeptide
PKA	protein kinase A
T2DM	type 2 diabetes mellitus
TC	cholesterol
TG	triglyceride
SCD1	stearoyl-coenzyme A desaturase 1
SREBP	sterol regulatory element binding protein
VPAC2	PACAP type III receptor
WAT	white adipose tissue
WT	wild type

impaired regulation of thermogenesis [11]. Site-specific injection of PACAP in the hypothalamus significantly increased energy expenditure of mice, and this effect was abolished by pretreatment with PACAP receptor PAC1 antagonisms [12,13]. Recent report showed that PACAP enhanced glucose-stimulating insulin secretion by increasing the levels of cAMP in rat pancreatic β-cells [14], activating leptin signaling pathways, and decreasing body weight in rats [15]. However, knowledge is limited about the underlying mechanisms that mediating the effect of PACAP on lipid metabolism.

In our previous study, we investigated the effect of PACAP in obesity, and found that PACAP ameliorated obesity through inhibiting hepatic inflammation. This effect of PACAP were mediated by Fas apoptosis inhibitory molecule (FAIM), which was originally discovered as the function of inhibiting fas-induced apoptosis [16,17]. FAIM plays an important role in multiple cellular processes including neuro-development, cell differentiation and apoptosis, and has various physiological functions such as maintaining metabolic homeostasis [18,19]. For example, FAIM protects against death receptor-triggered apoptosis and regulates B-cell signaling and differentiation. Besides, several reports indicated that FAIM protected cells by counteracting stress-induced cell death and regulating autophagy in lung adeno-carcinoma [20]. Moreover, studies have shown that knockout of FAIM inhibited the expression of insulin receptor β (IRβ) and impaired the insulin signaling pathway. FAIM inhibition results in spontaneous obesity and hepatic steatosis [21]. Besides, PACAP and FAIM were downregulated in the liver of HFD mice. While the expression of FAIM increased after PACAP treatment, we thus speculated that FAIM might mediated the beneficial effect of PACAP on reducing hepatic lipid accumulation, which provides insights into developing therapeutics against MAFLD.

2. MATERIALS AND METHODS

2.1. Animals and treatment

All animal experiments were approved by the Jinan University Animal Care and Use Committee. The animals received humane care according to the National Research Council's Guide for the Care and Use of Laboratory Animals. 4 weeks old C57BL/6J mice (male) were purchased from SPF (Beijing) biotechnology co., LTD. The mice were maintained in a specific pathogen-free environment and housed in groups of five animals per cage, in light/dark cycle (12 h/12 h) with a constant temperature of 20—25 °C and 45—60% humidity. Mice fed with a common diet (10% fat, 70% carbohydrate, 20% protein, D12450B, Research Diet, USA) or a high-fat diet (60% fat, 20% protein, 20% carbohydrate, D12492, Research Diet, USA). All mice had ad libitum access to food and sterile water. Animal weights and food intake were recorded weekly. After 8 weeks, mice were subjected to intraperitoneal administration of different doses of PACAP (0.2, 0.4, and 0.6 mg/kg, dissolved in physiological saline) or saline (served as a control) once daily for 4 weeks.

2.2. Lentivirus vector construction and infection

For FAIM knockdown or overexpression experiments, mouse *Faim* short-hairpin RNA (LV-shFAIM) or the entire coding region of the mouse FAIM gene [NM_011810.3] (LV-FAIM) were placed into a replication-defective lentiviral vector under the control of the U6 promoter or the cytomegalovirus promoter (Hanbio Biotechnology, CHINA). The scramble shRNA (LV-shCtrl) or control cDNA (LV-Ctrl) were used as control. The following lentiviral vectors were used: LV-shFAIM: pHBLV-U6-MCS-CMV-ZsGreen-PGK-Puro (size: 8991 bp). LV-FAIM: pHBLV-CMV-MCS-3flag-EF1-ZsGreen-T2A-Puro (size: 8974 bp). The sequences of the shRNAs are listed in Supplementary Table 1. For lentivirus infection in the HFD mouse model, HFD mice were injected with lentivirus (5×10^7 plaque-forming units) through the tail vein as described previously [16]. After 2 weeks, mice were sacrificed, blood samples, liver, and white adipose tissue were collected for further analysis, liver and white adipose weight were measured, the serum and liver were collected for detection of biochemical indexes.

2.3. Histological analysis

Mice liver and white adipose tissue from mice were fixed with 4% paraformaldehyde (MA0192, 30525-89-4, Meilunbio, China) overnight, embedded in paraffin (76242, 8002-74-2, Sigma, USA), and sectioned at 5 μm thickness and stained with hematoxylin-eosin (H&E) for histological analysis. Oil Red O staining (G1260, Solarbio, China) was performed on frozen sections using standard techniques.

2.4. Mouse metabolic assays

Mice were fasted for 12 h before blood glucose measurement. Tail vein blood glucose was measured with the use of a one-touch blood glucose measurement system (Sinocare blood glucose meter, CHINA). The serum lipid contents were measured using an automatic biochemical analyzer (Chemray 800, Rayto, CHINA) according to manufacturer's instructions. The fasting serum content of insulin was determined by ELISA (EM017-96, ExCell bio, CHINA). The homeostasis model assessment of insulin resistance (HOMA-IR) and HOMA-β were calculated by the following formula.

HOMA-IR index: [fasting blood glucose levels (mmol/l) × fasting serum insulin levels (μIU/ml)]/22.5. HOMA-β: [20 × fasting insulin (μIU/ml)]/[fasting glucose (mmol/l) − 3.5].

2.5. Intraperitoneal glucose tolerance test (IPGTT) and insulin tolerance test (IPITT)

Mice were fasted for 12 h (IPGTT) or 4 h (IPITT) prior to the tests. D-Glucose (2 mg/g, G8270, 50-99-7, Sigma, USA) or Insulin (0.75 unit/kg, R917753, 11061-68-0, Macklin, CHINA) was injected intraperitoneally. Then measure tail blood glucose at 0, 15, 30, 60, 90, 120 min following the injection. Area under the glucose—time curve (AUC) were calculated to quantify the IPGTT and IPITT results.

2.6. Cell culture and treatment

AML12 cell lines were obtained from ATCC. AML12 cells were cultured in DMEM/F12 medium (11330-032, Gibco, USA) supplemented with ITS supplement (I3146, Sigma, USA) and 40 ng/ml dexamethasone (D917754, 50-02-2, Macklin, CHINA); the medium was supplemented with 100 U/ml of penicillin, 100 μg/ml of streptomycin (15140-122, Gibco, USA) and 10% FBS (10099-141, Gibco, USA) at 37 °C in a humidified atmosphere of 95% air and 5% CO_2. For the *in vitro* experiments, cells were treated with 200 μM PA for 24 h to mimic lipid accumulation *in vitro*, then treated with 0.5 or 1 μM PACAP (52290, GL biochemicals, CHINA) in cell medium for another 24 h. Max.D.4 (GL biochemicals, CHINA) was used to block PACAP type 1 receptor (PAC1). AML12 were preincubated with Max.D.4 (10 μM) for 30 min before the treatment with PACAP (1 μM). To inhibit or activate the AMPK pathway, 10 μM Compound C (CC, S7840, 866405-64-3, Selleck Chemicals, USA) or 0.5 mM AICAR (S1802, 2627-69-2, Selleck Chemicals, USA) were administrated into the medium of the cell before PACAP treatment for 1 h. Primary mouse hepatocytes were isolated from C57BL/6J mice using the collagenase perfusion method as previously described [22].

Palmitate (P9767, 408-35-5, Sigma, USA) was coupled to BSA for the treatment *in vitro*. Palmitate was dissolved in double-distilled water with the heat at 70 °C, BSA (B-2064, 9048-46-8, Sigma, USA) was dissolved in sterile phosphate buffered saline (PH 7.2) at room temperature and incubated at 37 °C for 30 min prior to the addition of PA. The final concentration of PA stock solution is 10 mM (the final molar ratio of PA/BSA is 5:1).

2.7. RNA interference

2×10^5 AML12 cells were seeded into 6-well plates with 100 pmol FAIM siRNA by Lipofectamine 3000 (L3000008, Invitrogen, USA) as indicated protocols by the supplier. The knockdown efficiency was verified by qRT-PCR and western blotting. Three siRNAs of FAIM and a scrambled control were purchased from Ribobio (siBDM1999A, Guangzhou, CHINA, the sequences could be found in Supplementary Table 2, siFAIM-2 was chosen in the experiments). AMPK siRNA (targeting mouse AMPKα1: 5′-ACAUAUGCUGCAGGUGGA-3′, GenePharma, Shanghai, CHINA)

2.8. Plasmid constructs and dual luciferase assay

The mouse FAIM proximal promoter genomic region (NC_000075.7:98866745-98868446 as described in the National Center for Biotechnology Information database, −1681 to +20, −520 to +20 and the CRE element mutant promoter-reporter constructs −1681 to +20) were inserted upstream of a luciferase reporter gene with a flanking sequence into the BglII and apal-digested pmirGLO (E1330, Promega) vector to generate pmirGLO-FAIM (WT, mutant, truncated), respectively. The coding region of the mouse Creb1 gene (*Mus musculus*, transcript variant C, NM_001037726.1) was cloned into the pcDNA3.1(+) vector (pcDNA3.1(+)-CREB). The plasmids were constructed and sequenced by Genewiz (Suzhou, CHINA). AML12 were transfected with FAIM promoter-luciferase reporter plasmids and pcDNA3.1(+)-CREB vector using Lipofectamine 3000 according to the manufacturer's instructions. In CREB inhibitor experiment, AML12 were transfected with FAIM reporter plasmids for 24 h and treated with 1 μM PACAP for an additional 24 h in the presence or absence of the CREB inhibitor KG-501 (S8409, 18228-17-6, Selleck Chemicals, USA). Cells then lysed in 100 μl lysis buffer and detected using the Dual-Luciferase Reporter Assay System (E1910, Promega). Renilla luciferase activity was used as a control.

2.9. Triglyceride and total cholesterol measurement

The triglyceride (TG) and total cholesterol (TC) levels of cells and liver tissue were measured using triglyceride and total cholesterol quantification assay kits (A110-1-1for TG, A111-1-1 for TC, Nanjing Jiancheng Institute, CHINA). Briefly, cells were rinsed with PBS and digested with 0.25% trypsin (25200-056, Gibco, USA). After centrifuge, cell pellets were lysed with cell lysis buffer that contained a protease and phosphatase inhibitor cocktail (P1050, Beyotime, CHINA). The content of TG and TC were determined according to the manufacturer's instructions and total protein concentrations were quantified by the BCA method for normalization (23227, ThermoFisher scientific, USA). Frozen liver samples (20 mg) were homogenized in RIPA buffer (P0013B, Beyotime, CHINA) and TG and TC levels were determined according to the manufacturer's instructions.

2.10. Glucose uptake and glycogen content assay

Glucose uptake of AML12 was evaluated by using 2-NBDG (11046, 186689-07-6, Cayman, USA). The assay was performed based on previously published methodology [23], with slight modifications. Briefly, AML12 cells were cultured in glucose-free DMEM/F12 medium, treated with different stimuli for 48 h to evaluate the glucose uptake, the treatment was followed by insulin (100 nM) for 30 min, and 2-NBDG (100 μg/ml) for 2 h incubation at 37 °C. Next, the cells were gently rinsed with glucose-free Krebs Buffer (120 mM NaCl, 5 mM KCl, 2 mM $CaCl_2$, 1 mM $MgCl_2$, 25 mM $NaHCO_3$; at pH 7.2). Then the medium was replaced with glucose-free Krebs buffer and incubated for 10 min. The supernatant was aspirated, 100 μl glucose-free Krebs buffer was added to each well and the fluorescence intensity was quantitated with a multi-functional microplate reader (excitation/emission wavelengths = 485/535 nm). The glycogen content was estimated by glycogen assay kit (BC0345, Solarbio, CHINA) following the manufacturer's approach, and normalized with the cell amount.

2.11. qRT-PCR

Total RNA was extracted using RNAiso reagent according to the manufacturer's instructions (9109, Takara, JAPAN). For RT-PCR, mRNA was reverse transcribed into cDNA using the ReverTra Ace qPCR RT Master Mix with genomic DNA remover (FSQ301, Toyobo, JAPAN), and cDNA was amplified by quantitative real-time PCR (qPCR) using 2x SYBR Green qPCR Master Mix (B21203, Bimake, CHINA) and normalized to β-actin. The sequences of the primers are listed in Supplementary Table 3.

2.12. Western blot

The primary antibodies used in this study are FAIM(Ab154570, Abcam), IRβ (3025, Cell Signaling Technology), Phospho-IRβ (3021, Cell Signaling Technology), AMPK (2532, Cell Signaling Technology), Phospho-AMPK (2535, Cell Signaling Technology), FAS (3180, Cell

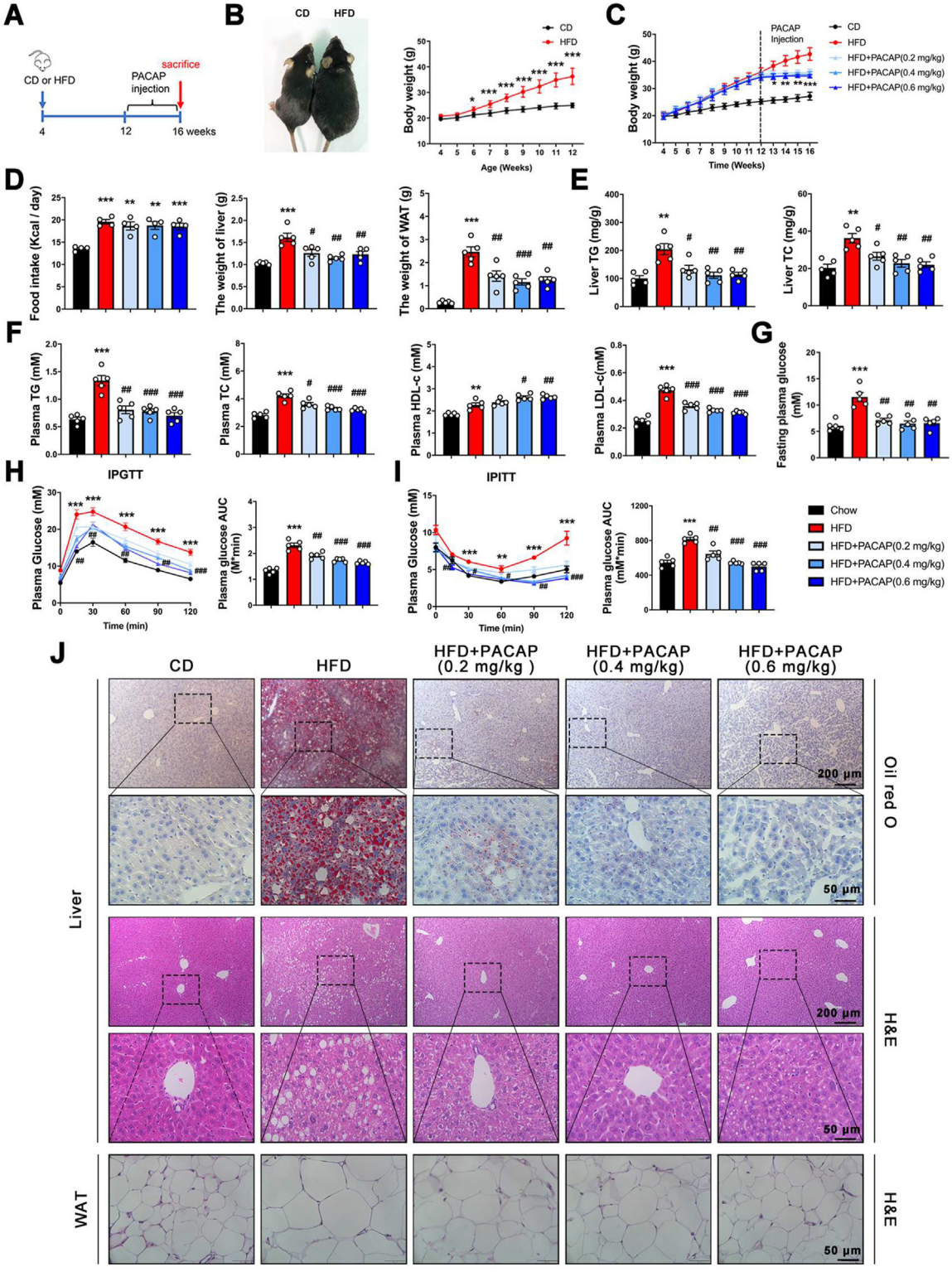

Figure 1: PACAP improves HFD-induced hepatic lipid accumulation and insulin sensitivity in mice. (A) Schematic diagram of HFD induced mouse model with PACAP injection. Male C57BL/6J mice at 4 weeks of age were randomly grouped (n = 5), allowed ad libitum access to different diets (chow diet and high-fat diet) and water. Vehicle (saline solution), PACAP (0.2, 0.4, or 0.6 mg/kg) was administrated to mice by intraperitoneal injection once per day for 4 weeks and then mice were sacrificed and subjected to a series of analyses as indicated below. (B) General appearance and bodyweight of CD group and HFD group. (C) Bodyweight, (D) Food intake, liver weight and WAT weight in mice at 16 weeks (n = 5). (E–G) The effect of PACAP on liver TG and TC (E), plasma TG, TC, HDL-C, and LDL-c levels(F) and fasting blood glucose(G). (H and I) IPGTT (H) and IPITT (I) in HFD mice 4 weeks after PACAP treatment; quantification of area under curve in IPGTT and IPITT (right). (J) Oil Red O staining and H&E staining of mouse liver and WAT section. Data are presented as mean ± SEM ($^{*}P < 0.05$, $^{**}P < 0.01$, $^{***}P < 0.001$ *vs.* CD group; #$P < 0.05$, ##$P < 0.01$, ###$P < 0.001$ *vs.* HFD group, n = 5 per group).

Signaling Technology), ACC (3662, Cell Signaling Technology), Phospho-ACC (11818, Cell Signaling Technology), HMGCR (Ab174830, Abcam), SREBP1 (Ab3259, Abcam), SREBP2 (Ab30682, Abcam), SCD1 (Ab19682, Abcam) and β-actin (8H10D10, Cell Signaling Technology). Cells were harvested and lysed in RIPA buffer containing a protease and phosphatase inhibitor cocktail; tissue samples were homogenized with a tissue homogenizer in RIPA buffer. Protein samples concentration was determined using the BCA protein assay kit (23227, ThermoFisher scientific, USA) as described previously [24]. Proteins were separated on 8—12% SDS-PAGE gels and transferred to PVDF membranes (0.22 μm, PALL, USA). The membranes were blocked for 1 h at room temperature with 5% BSA (SRE0096, Sigma, USA) in TBS-T (Tris-buffered saline (50 mM Tris, 150 mM NaCl, pH 8.0) containing 0.1% Tween 20). Next, the membranes were incubated with the primary antibodies at 4 °C overnight. After that, the membranes were washed and incubated with an appropriate HRP-conjugated secondary antibody at room temperature for 1 h. The protein bands were visualized with a Super Lumia ECL Plus HRP substrate kit (BMU101-CN, Abbkine, USA). Densitometric quantification analysis was determined using an Image Lab analysis system (Bio-Rad, USA).

2.13. Statistical analysis

Statistical analysis was performed by GraphPad Prism. All quantification data are presented as mean ± SEM. Statistical analysis was calculated by two-tailed Students' *t*-test. Significance was considered when $P < 0.05$.

3. RESULTS

3.1. PACAP ameliorates HFD-induced obesity, hepatic lipid accumulation, and improves insulin sensitivity in mice

In this study, 4 weeks old mice were fed with a high-fat diet (HFD) to induce obese models (Figure 1A). The HFD-fed mice exhibited a significant increase in body weight compared to Chow diet (CD)-fed mice after two weeks (Figure 1B). After 8 weeks of different feeding, PACAP was intraperitoneally injected into the HFD-fed mice for additional 4 weeks. PACAP treatment decreased the body weight in HFD-fed mice (Figure 1C). No significant difference in food intake were observed in different groups. Meanwhile, PACAP administration markedly decreased the weight of liver and white adipose tissue (WAT) in HFD-fed mice (Figure 1D).

The effects of PACAP on lipid metabolism in HFD-fed mice were studied by measuring the plasma lipids and liver TG/TC levels. PACAP administration decreased the plasma TG, TC, and low-density lipoprotein cholesterol (LDL-c) levels. In addition, PACAP further increased the high-density lipoprotein cholesterol (HDL-c) level induced by HFD (Figure 1F). Moreover, PACAP treatment dramatically decreased the liver TG and TC contents of HFD-fed mice by 40—80% (Figure 1E). Hepatic lipid accumulation was also observed by histological analysis of liver and white adipose tissue. The results showed that PACAP effectively reduced lipid droplets accumulations in the liver sections of HFD-fed mice, and the medium dose PACAP (0.4 mg/kg) exhibited the better therapeutic effect (Figure 1J). The results indicated that HFD-fed mice exhibited hepatic lipid accumulation, which was repressed by PACAP treatment.

On the other hand, the effect of PACAP on glucose tolerance and insulin sensitivity were explored by IPGTT and IPITT. The results showed that PACAP treatment exerted beneficial effects on HFD-induced glucose intolerance (Figure 1H,I). Furthermore, PACAP recovered the impairment of fasting blood glucose and fasting serum insulin content in HFD mice (Figures 1G and S1A). PACAP improved the insulin sensitivity of HFD mice, which is also demonstrated by the homeostasis model assessment of insulin resistance (HOMA-IR) index (Figure S1B). Besides, islet β-cell function, calculated by HOMA-β formular, also showed improvement after PACAP administration (Figure S1C). All together, these results demonstrated that PACAP treatment ameliorates HFD-induced obesity, hepatic lipid accumulation and improves insulin sensitivity in HFD-fed mice.

3.2. PACAP promotes the activation of the AMPK and IRβ and decrease the expression of lipogenesis genes both *in vivo* and *in vitro*

We sought to explore the molecular mechanism underlying the beneficial effects of PACAP administration. It has been reported that PACAP/cAMP canonical pathway caused LKB1-mediated AMPK activation during PACAP-stimulated neuroendocrine cell differentiation [25]. AMPK is a central mediator of metabolism that regulates a series of lipogenesis genes expression. Hence, the activation of key members of AMPK pathway, PI3K-Akt pathway, and lipogenesis genes was checked by western blot. Our results showed that the PACAP administration increased the phosphorylation of AMPK (Thr172), IRβ (Thr1146), and Akt (Ser 473) in the livers of HFD-fed mice (Figure 2A). Moreover, PACAP treatment reduced protein levels of the matured forms of SREBP1 and SREBP2, two key transcriptional factors that regulate lipogenesis. Accordingly, PACAP downregulated the protein levels of SREBP's downstream genes SCD1, FAS, and HMGCR in the livers of HFD mice (Figure 2B). Additionally, we tested the phosphorylation level of AMPK and the content of TG in mice skeletal muscle (Figure S2A). The results showed that the TG contents in skeletal muscle of PACAP-treated HFD mice were not significantly decreased (Figure S2B). Moreover, PACAP reduced the transcriptional level of lipogenesis genes in white adipose tissues of HFD mice (Figure S2C).

To confirm the effect of PACAP on AMPK-IRβ pathway, hepatocytes were incubated with palmitic acid (PA) and treated by PACAP *in vitro.* The results show that PACAP treatment markedly reduced lipid accumulation and intracellular TG and TC levels in PA-induced AML12 cells (Figure S3A—C). Furthermore, PACAP increased glucose uptake and glycogen content by 20—30% in the PA-induced AML12 cells (Figure S3D). However, Max.D.4, an antagonist of PACAP receptor PAC1, abolished the beneficial effects of PACAP (Figure S3A—D). At the same time, PACAP activated the AMPK-IRβ pathway and reduced the expression of genes related to lipid synthesis pathway in PA-treated AML12 cells (Figure 2C,D). Similar results were repeated in PA-treated primary mouse hepatocytes (Figure S4A,B). These results confirm our *in vivo* data and indicate that PACAP activates AMPK-IRβ pathway to inhibits lipogenesis gene expression in hepatocytes.

3.3. PACAP attenuates lipogenesis through the AMPK-IRβ pathway

We further demonstrated that AMPK plays a critical role in the therapeutic efficiency of PACAP in overnutrition-induced lipid accumulation. To do this, AML12 cells were treated with 10 μM Compound C (an AMPK inhibitor) or transfected with AMPK siRNA. The results show that inhibition of AMPK abrogated the effects of PACAP on IRβ phosphorylation and lipogenic gene expression (Figures 3A,B and S5A,B). On the other hand, activation of AMPK with AICAR (0.5 mM) simulated the effects of PACAP to further increase the phosphorylation of IRβ and downregulate the expression of lipogenesis genes (Figure 3C,D). Together, these results further support the idea that PACAP activates AMPK-IRβ pathway to decrease the expression of lipid synthetic genes.

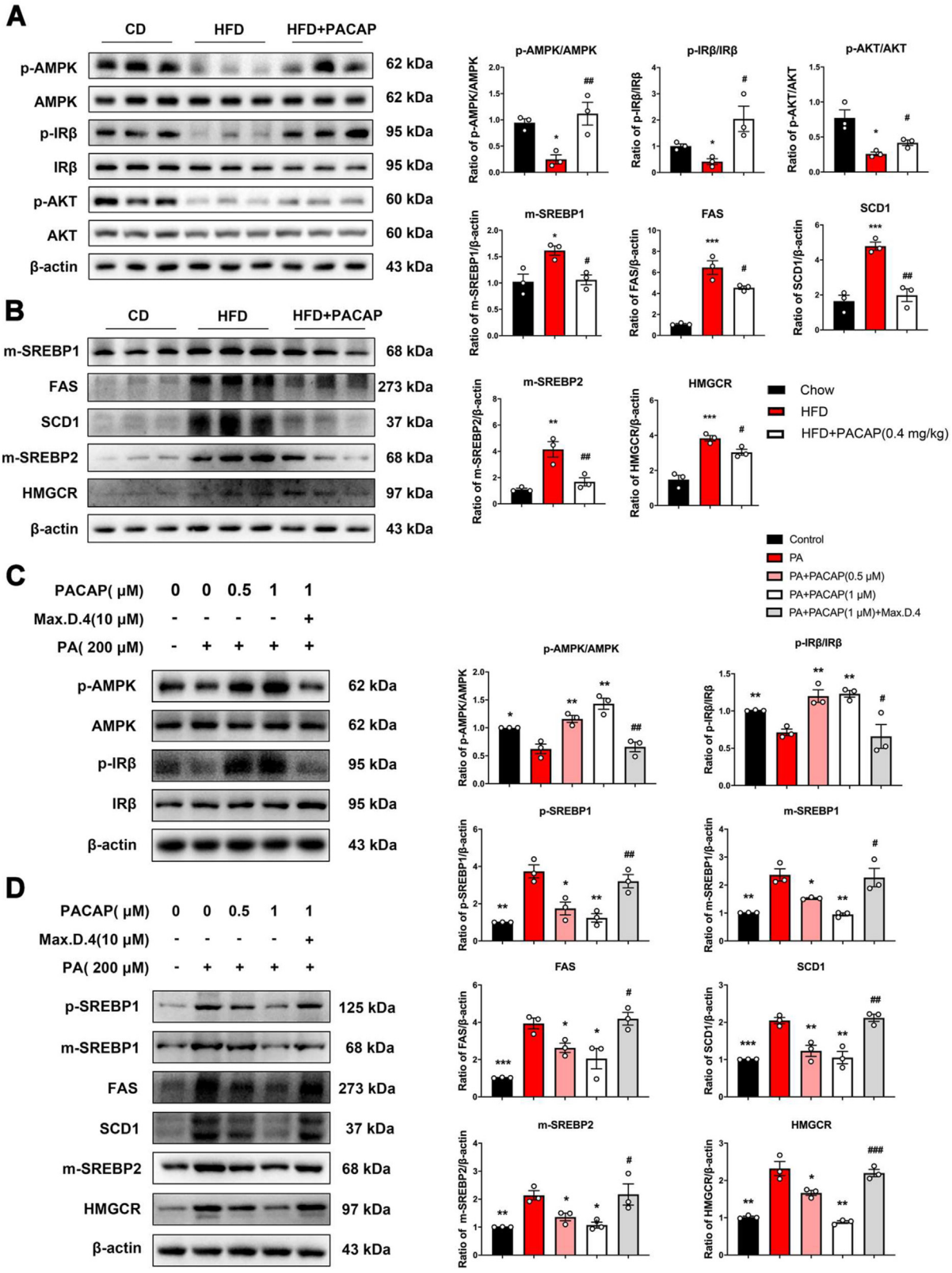

Figure 2: PACAP promotes the phosphorylation of AMPK and IRβ and decrease the lipogenesis gene expression both in vivo and in vitro. (A and B) Mice were sacrificed, and protein was extracted from liver tissues for western blot. Representative protein levels of p-AMPK, p-IRβ and AMPK downstream lipogenesis pathway were subjected to western blot with indicated antibodies and statistical analysis ($^{*}P < 0.05$, $^{**}P < 0.01$, $^{***}P < 0.001$ *vs.* CD group; $\#P < 0.05$, $\#\#P < 0.01$, $\#\#\#P < 0.001$ *vs.* HFD group). (C and D) AML12 were treated with PA (200 μM) 24 h to induce lipid accumulation model, then treated with PACAP (0.5 or 1 μM) or Max.D.4 (10 μM) for another 24 h, whole-cell extract underwent western blots with indicated antibodies. p-SREBP1 represents precursor SREBP1; m-SREBP1 or m-SREBP2 represents mature SREBP1 or SREBP2 ($^{*}P < 0.05$, $^{**}P < 0.01$, $^{***}P < 0.001$ *vs.* PA group; $\#P < 0.05$, $\#\#P < 0.01$, $\#\#\#P < 0.001$ *vs.* PACAP (1 μM) group); data are presented as mean ± SEM, n = 3.

3.4. FAIM mediates the effect of PACAP on AMPK activation *in vivo* to improve hepatic lipid accumulation and insulin sensitivity

Hepatic lipid accumulation induced by overnutrition causes sustained lipid stress in hepatocytes and contributes to the progression of MAFLD [1]. Our previous study showed that PACAP and FAIM levels in blood leucocytes are lower in obese persons [16]. Consistently, the expression level of FAIM was decreased in livers of HFD-fed mice, and PACAP reversed the downregulation of FAIM induced by HFD diet (Figure 4A). The results implicate a potential role of FAIM in mediating the effects of PACAP.

To test of this hypothesis, lentivirus encoding *Faim* shRNA (LV-shFaim) was used to downregulate FAIM expression in HFD mice with or without PACAP treatment (Figure 4B). Briefly, HFD-fed mice were treated with PACAP or mock for 4 weeks. The mice were then injected with LV-shFaim or control shRNA lentivirus (LV-shCtrl) through the tail vein. After another 2 weeks, mice were sacrificed and analyzed. *Faim* mRNA levels were decreased by 70–75% in the livers of shFaim injected mice compared to the control mice (Figure 4C). Metabolic phenotypes were examined after the injection. In PACAP-treated group, Faim knockdown significantly increased the weight of body, liver and WAT (Figure 4D). Meanwhile, the concentration of TG and TC in liver and plasma were increased significantly, with a decrease of plasma HDL-c (Figure 4E,F). Further, Faim knockdown in PACAP-treated group showed higher hepatic lipid accumulation in experiment staining of liver sections for total lipids with Oil Red O and H&E staining (Figure 4H). Likewise, knockdown of FAIM significantly increased fasting blood glucose level (Figure 4G) in parallel with impaired glucose tolerance and insulin sensitivity reflected by IPGTT (Figure 4I) and IPITT (Figure 4J). All changes with LV-shFaim were significant only in the PACAP-treated but not in mock-treated groups. These results suggest that FAIM mediates the effects of PACAP on obesity and fatty liver in HFD-fed mice.

We further examine whether FAIM mediates the effects of PACAP in activating AMPK-IRβ pathway and causing subsequent changes with western blot. Our results showed that knockdown of FAIM in PACAP-treated HFD mice weakened the activation of AMPK-IRβ signaling pathway and up-regulated lipid metabolism pathways. PACAP reduced the expression of lipogenesis genes in HFD mice, but FAIM knockdown suppressed the effects. The results suggested that the deficiency of FAIM counteracted the activation of AMPK and IRβ, as well as the reduced expression of lipid synthesis genes expression induced by PACAP treatment (Figure 5A,B). These results indicated that the ablation of FAIM weakens the effect of PACAP on the activating of AMPK-IRβ pathway in HFD-fed mice.

3.5. FAIM overexpression activated AMPK-IRβ signaling in HFD mice

A key result from our observations is that the expression level of FAIM and the phosphorylation of AMPK were up-regulated in the HFD-fed mice with PACAP administration. To verify the role of FAIM in mediating the activation of AMPK, the FAIM overexpression mice model was established through tail vein injection with lentivirus encoding FAIM cDNA (Figure S6A). After 2 weeks of injection, FAIM expression was increased significantly in the livers of HFD mice compared with the control littermates (with lentivirus-control cDNA) at the mRNA level (Figure S6B). Compared with the control group, overexpression of FAIM decreased bodyweight, liver weight, plasma lipids contents, fasting blood glucose, liver TG and TC (Figure S6C–G). Consistently, FAIM overexpression improved hepatic lipid accumulation (Figure S6H). Moreover, glucose tolerance was improved with FAIM overexpression in HFD-fed mice (Figure S6I). However, insulin sensitivity seemed not to improve in FAIM overexpression mice that were not treated with PACAP but significantly improved only in PACAP-treated groups. The possible explanation is that the effect of insulin sensitivity was mainly regulated by PACAP not just FAIM (Figure S6J).

Detailed analysis showed that FAIM overexpression increased the protein levels of phosphorylated AMPK and phosphorylated IRβ level and reduced the expression of key genes relating to lipogenesis. Moreover, the effects of FAIM overexpression were similar and additive to PACAP administration (Figure 5C,D). Altogether, our results demonstrated that upregulation of FAIM mediated the effect of PACAP in activating AMPK-IRβ pathway to protect mice from hepatic lipid accumulation.

3.6. FAIM knockdown weakened the activation of AMPK pathway *in vitro*

Next, we further verified *in vitro* that FAIM functions upstream of AMPK pathway in PA-induced AML12 cells. Transfection of FAIM siRNA (si-FAIM) increased lipid accumulation, intracellular TG and TC in PA-induced AML12 cells independent of PACAP treatment. Moreover, knockdown of FAIM reduced glucose uptake and glycogen contents in both PACAP-treated and mock cells (Figure 6A and C). Furthermore, knockdown of FAIM reversed the PACAP-induced activation of AMPK and IRβ (Figure 6D). Concurrently, FAIM-siRNA significantly upregulated the expression of lipogenic genes and neutralized the effects of PACAP treatment (Figure 6E).

On the other hand, the expression of FAIM didn't increase in AML12 cells treated with AICAR, an AMPK activator (Figure 6F). Correspondingly, suppression of AMPK activity with CC treatment or AMPK siRNA did not alter the expression of FAIM (Figures 6G and S5A). These results further support that AMPK functions as a downstream mediator of FAIM. Interestingly, the expression of FAIM in PA-induced AML12 was upregulated after the treatment of AICAR, which may be secondary to the effect of AICAR on the improvement of lipid metabolism. Together, FAIM deficiency impaired the effect of PACAP on activating the FAIM-AMPK-IRβ axis and decreasing lipid accumulation *in vitro*.

3.7. PACAP regulates the expression of FAIM by promoting the transcriptional activity of the *Faim* promoter

We further explored the mechanism through which PACAP upregulated FAIM expression. We first analyzed the upstream promoter sequence of the *Faim* gene using the TRAP tool and JASPAR database for predicting the transcription factor binding sites [26,27]. Transcription factors (E2F, EGR3, CDP, CREB, ATF5, HMX3, OCT1, IRF8, CHOP, LEF1, MEF2, SMAD3, etc.) had putative binding sites in the promoter regions of *Faim* gene. Of these, CREB1 was of special interest as CREB is downstream of the classical PACAP/PKA signaling pathway. CREB1 is a member of the leucine zipper family of DNA binding proteins. Two consensus binding sites derived from a Positional Weight Matrix in the JASPAR database of CREB were found in the upstream regions of *Faim*.

We determined the phosphorylation of PKA and CREB, and the expression level of FAIM by western blot after treating PA-induced AML12 cells with PACAP. The result showed that PACAP upregulated p-PKA, p-CREB, and FAIM levels (Figure 7A,B). Next, we performed a dual-luciferase reporter assay to investigate the effect of PACAP on the *Faim* promoter. Two predicted CREB1 binding sites located between −1681 and −520 bp upstream of the transcription start site (TSS) in the FAIM promoter were identified by using the JASPAR database, and the two sites were labeled as "A" (AGACCTCA, −1390/−1382) and "B" (CGACCTCA, −597/−589). Three *Faim* promoter luciferase reporter plasmids, including full length

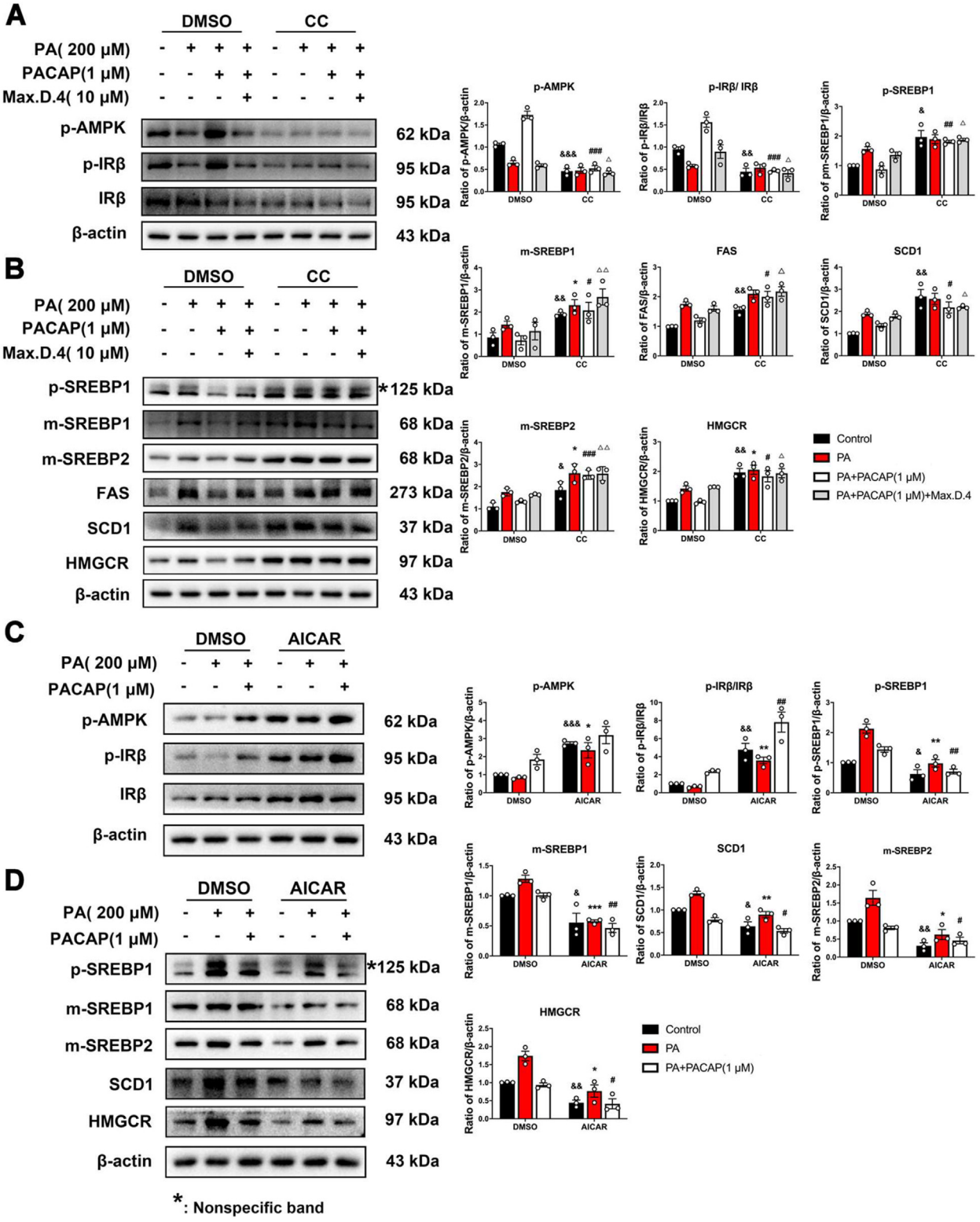

Figure 3: PACAP reduced lipogenic gene expression through the AMPK-IRβ pathway. (A and B) AML12 were exposed to PA for 24 h, then treated with PACAP (1 μM), Max.D.4 (10 μM), and Compound C (10 μM) for another 24 h. Representative protein levels were detected by western blot analysis. (C and D) AML12 were exposed to PA for 24 h then treated with PACAP (1 μM), and AICAR (0.5 mM) for another 24 h. Representative protein levels were detected by western blot analysis. The quantification of protein level was showed in a bar chart (right). Data are presented as mean ± SEM. (&$P < 0.05$, &&$P < 0.01$, &&&$P < 0.001$ *vs.* control group; *$P < 0.05$, **$P < 0.01$, ***$P < 0.001$ *vs.* PA group; #$P < 0.05$, ##$P < 0.01$, ###$P < 0.001$ *vs.* PA + PACAP group, △ $P < 0.05$, △ △ $P < 0.01$, △ △ △ $P < 0.001$ *vs.* PA + PACAP + Max.D.4 group; n = 3).

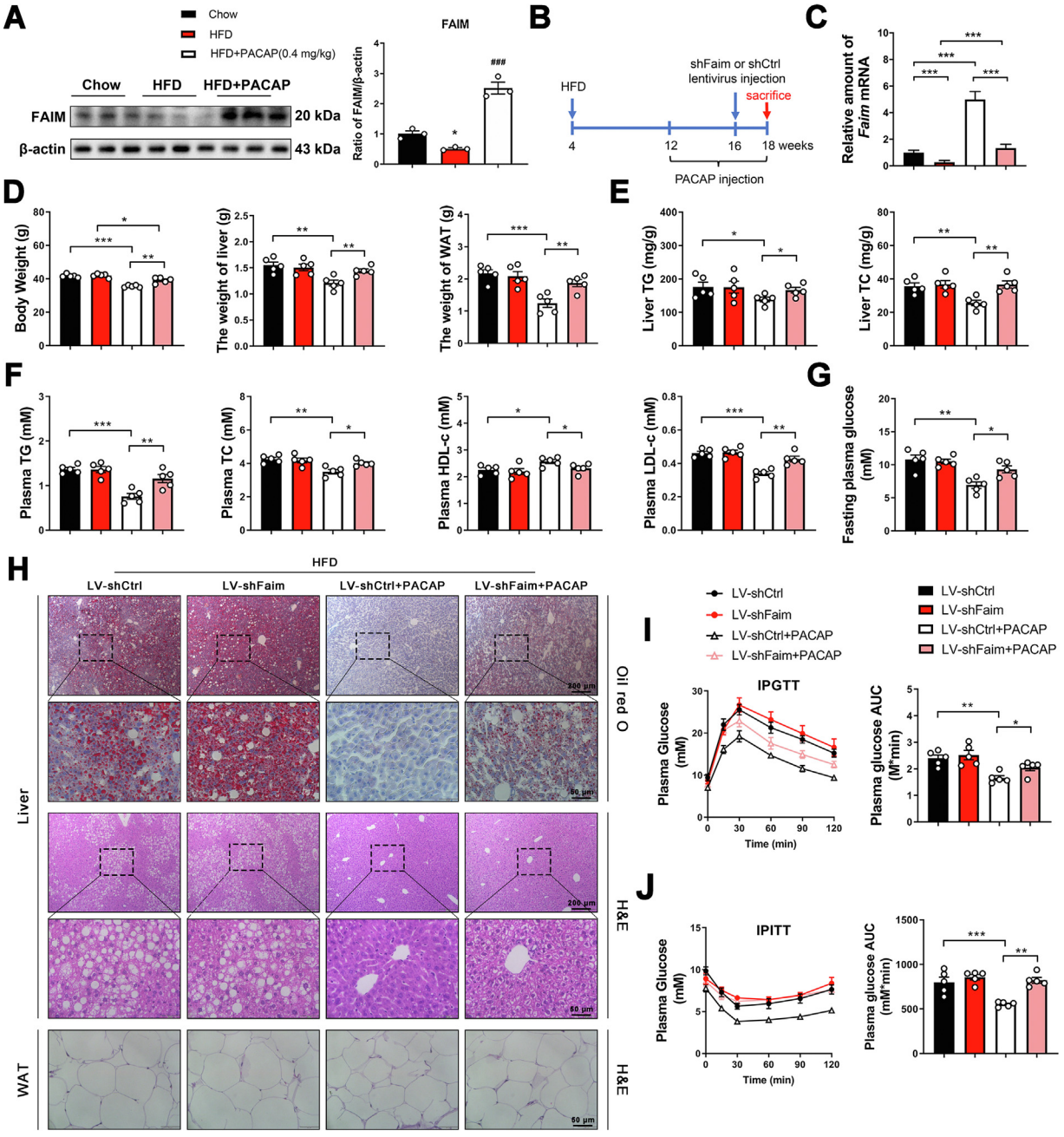

Figure 4: FAIM deficiency suppressed the effects of PACAP on alleviating hepatic lipid accumulation in HFD-fed mice. (A) FAIM protein level of mice liver was subjected to western blot. Statistical analysis of FAIM/β-actin was shown in a bar chart (right) (*$P < 0.05$, **$P < 0.01$, ***$P < 0.001$ *vs.* CD group; #$P < 0.05$, ##$P < 0.01$, ###$P < 0.001$ *vs.* HFD group). (B) Schematic diagram of HFD mouse model with PACAP treatment (0.4 mg/kg) or control saline solution and lentivirus mediated *Faim* knockdown. (C) Hepatic *Faim* mRNA level was determined by qRT-PCR, n = 3. (D–H) Modulation of *Faim* level in the liver influenced HFD-induced hepatic steatosis, (D) bodyweight, liver weight, and WAT weight; (E) liver TG and TC contents; (F) plasma TG, TC, HDL-c, and LDL-c levels; (G) fasting blood glucose level; blood glucose concentrations were measured on day 12 after lentivirus injection; (H) representative photomicrographs of Oil Red O and H&E staining of liver tissues in different groups (scale bars: 50 or 200 μM). (I and J) Ablation of *Faim* impaired glucose tolerance and insulin sensitivity in mice. IPGTT (I) and IPITT (J), blood glucose was measured at different time points after glucose or insulin injection (left), and quantification of the AUC (right). Data are presented as mean ± SEM, n = 5 (*$P < 0.05$, **$P < 0.01$, ***$P < 0.001$).

(−1681 to +20), truncated type (−520 to +20), and mutant type were constructed (−1681 to +20, mutate both sites A and B as AGACAGCA and CGACAGCA, schematic diagram of constructs in Figure 7C). These reporter plasmids, including empty vector, were separately transfected into AML12 cells. The transcriptional activities were analyzed using a dual-luciferase reporter system. The results showed that the truncated and the mutation constructs significantly reduced luciferase activity compared to the full-length vector (by 4.5-fold and 2.5-fold respectively) (Figure 7D). This result revealed that the two CREB binding sites region between −1681 and −520 could regulate *Faim* expression.

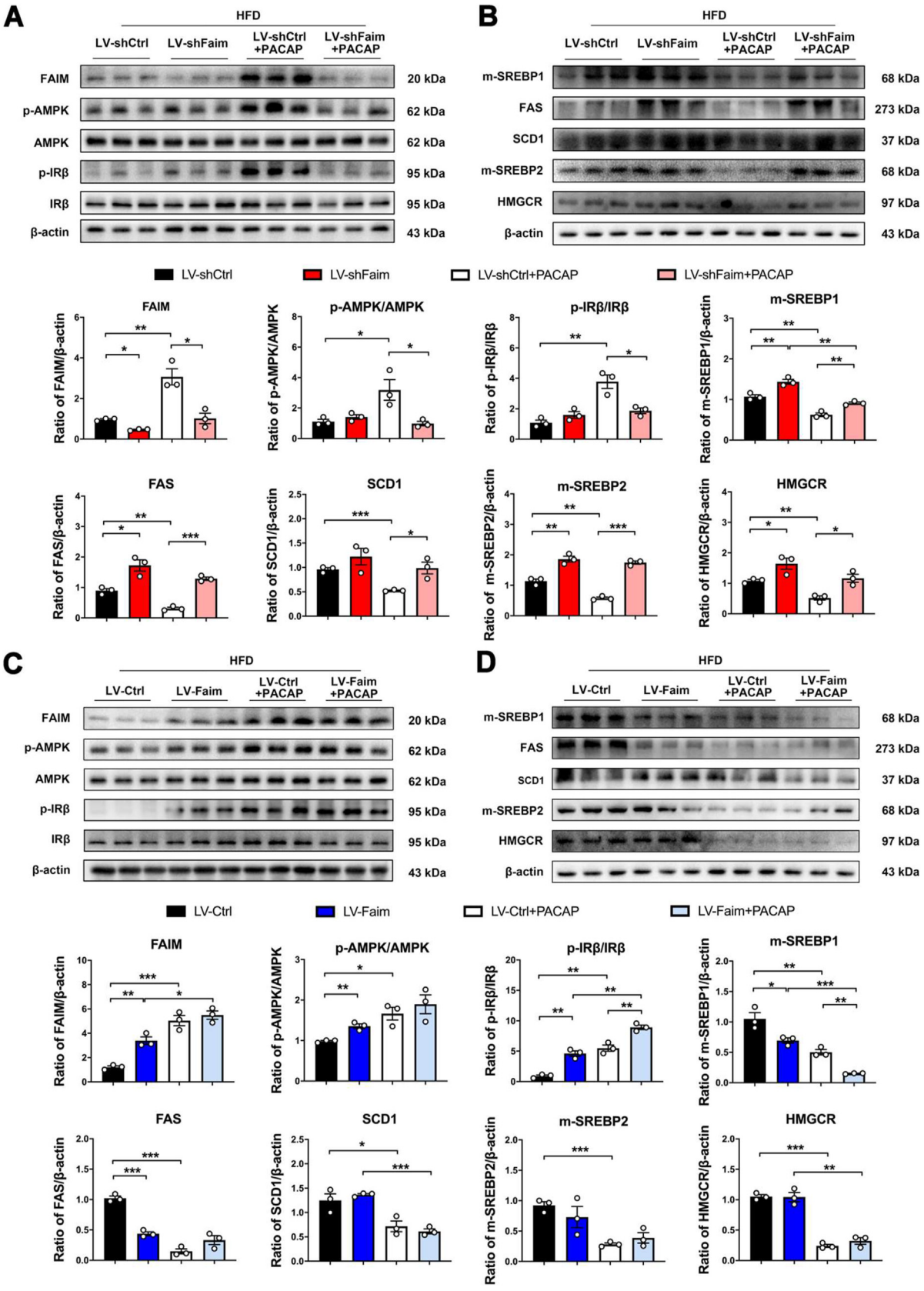

Figure 5: PACAP activates the FAIM-AMPK-IRβ axis to govern the SREBP and lipid synthetic gene program. (A and B) PACAP activated AMPK-IRβ signaling pathway and down-regulated the expression of lipogenesis genes in HFD-fed mice, such effects were suppressed following knockdown of *Faim*. Western blot analysis were used to detect the protein level of indicated antibodies. (C and D) The overexpression of FAIM activated AMPK-IRβ signaling pathway, the protein levels of FAIM, p-AMPK, AMPK, p-IRβ, IRβ, and lipid synthesis genes SREBP1, SREBP2, FAS, SCD1, HMGCR were determined by western blot with quantifications. Data are presented as mean ± SEM, n = 3 ($^{*}P < 0.05$, $^{**}P < 0.01$, $^{***}P < 0.001$).

Next, we investigated whether PACAP regulated the FAIM transcriptional activity through CREB binding sites. AML12 cells were treated with PACAP or co-transfected with CREB cDNA expression plasmid and empty vectors. PACAP treatment strongly activated upregulated luciferase activity of the wildtype FAIM promoter but not mutated or truncated promoter (Figure 7E). Similar effects were shown with CREB overexpression (Figure 7F). Moreover, KG-501 (a specific CREB inhibitor) strongly decreased *Faim* promoter luciferase activity and blocked the increasement by PACAP (Figure 7G). These findings indicated that PACAP improves *Faim* expression via promoting the transcriptional activity of the *Faim* promoter through CREB.

Overall, our study provided evidence that PACAP has therapeutic effect of fatty liver phenotypes through the activation of FAIM-AMPK-IRβ axis to reduce the *de novo* lipogenesis gene expression.

4. DISCUSSION

The rising prevalence of metabolic risk factors among MAFLD patients underlines the imperative requirement for novel therapeutic strategies. One potential therapeutic strategy for treating MAFLD is to alleviate hepatic lipid accumulations [28]. The effective reduction of metabolic stress by repressing lipogenesis represents a beneficial approach for treating MAFLD. Thus, we aimed to investigate the therapeutic effect of PACAP on hepatic lipid accumulation. Our results focused on the metabolic effects of PACAP through activating FAIM-AMPK-IRβ axis in the context of overnutrition-induced metabolic disorders. Our data demonstrated the efficacy of PACAP in regulating of lipid metabolism through decreasing lipogenesis under HFD feeding, and that FAIM mediated the effect of PACAP in activating AMPK and the reducing lipogenic gene expression. Collectively, our data suggest that PACAP protects hepatocytes from lipid stress, which provided the potential role of PACAP in preventing or treating metabolic disorders including MAFLD.

PACAP is a bioactivity neuro-activating polypeptide, which plays important roles in many biological processes, including neurodevelopment, embryogenesis, cell proliferation, differentiation, and apoptosis. Accumulating studies demonstrated the roles of PACAP in energy homeostasis [9,12,29]. Previous studies have reported that PACAP treatment inhibited oxidized low-density lipoproteins-induced intracellular lipid storage *in vitro*, and endogenous PACAP protected mice pancreatic β-cells from lipotoxicity in mouse model [30,31]. As a member of the glucagon superfamily, PACAP has a significant effect on insulin secretion. It was reported that administration of PACAP promotes insulin secretion and reduce glucose levels in animal models with diabetes or glucose intolerance [9,32].

Based on the pathogenesis of MAFLD, numerous compounds and drugs are currently under investigation for treating MAFLD, while some of them were under phase III clinical trials [33]. GLP-1 is a member of the PACAP/glucagon superfamily with anti-diabetic effects, and GLP-1 receptor agonists are a class of drugs with multifactorial effects [34]. GLP-1 analogs and GLP-1 receptor agonists were designed and optimized to replace GLP-1 with subcutaneous, sublingual or oral administration. A clinical trial of semaglutide, a GLP-1 receptor agonist, reported that 59% of patients with resolved non-alcoholic steatohepatitis (NASH) and no worsening of fibrosis [35]. In addition to the effects of improving glucose and lipid metabolism [36], GLP-1 receptor agonists were also shown to reduce the risk of adverse cardiovascular events [37]. However, it could also inhibit gastric emptying and food intake and cause severe gastrointestinal events, including nausea, diarrhea, and vomiting [38,39].

Compared to GLP-1 receptor agonists, PACAP showed gastrointestinal protection. Studies reported that PACAP was involved in pathogenesis within the gastrointestinal tract, including inflammation, diabetes, cancer, and intoxication [40]. Like GLP-1, the main problem in the therapeutic effect of PACAP is the rapid degradation, with its half-life less than 5 min in blood. BAY55-9837, an agonist of PACAP receptor VPAC2, was developed as a potential therapeutic peptide in treating T2DM [41]. However, the therapeutic effect of BAY55-9837 was limited due to its short half-life, lacking of targeting ability, and poor blood glucose response. Some studies identified a series of conformationally restricted analogs of PACAP through structure-function study, or designed a derivative of PACAP that behaves as a superagonist towards the PAC1 receptor [42,43]. Other researchers modified the PACAP peptide by using site-directed mutagenesis, by medicinal chemistry approaches to make it into a recombinant slow-released peptide, or combined with magnetic nanoparticles or other biomaterials to improve the half-life, stability, bioavailability, or *in vivo* efficacy [44,45]. PACAP and its receptor agonists are of great interest in the treatment of metabolic disorders including T2DM and MAFLD, however, the application of PACAP receptor agonists in the treatment of metabolic diseases needs further study.

In this study, our data showed that PACAP improved hepatic lipid metabolism and reduced hepatic lipid accumulation with decreased body weight and increased insulin sensitivity in HFD-fed mice. We also demonstrated that PACAP activated the AMPK-IRβ signaling pathway in the liver of HFD-fed mice through regulating FAIM. The result suggested that PACAP activated FAIM to ameliorate overnutrition-induced metabolic disorders. FAIM is an anti-apoptotic protein, which is evolutionarily conserved [18]. There are two isoforms of FAIM, the longer isoform is mainly expressed in the nervous system, and the short isoform is ubiquitously expressed which is studied here. Emerging data demonstrated that FAIM was also involved in multiple cellular and physiological functions [46–49]. Our study showed that knockdown of FAIM resulted in hepatic steatosis and impaired insulin signaling pathway, which is consistent with our previous study in FAIM knockout mice [21]. Our results also suggested that the activation of FAIM in liver showed beneficial effects on overnutrition induced metabolic disorders, which was likely due to its role in decreasing the expression of lipogenic genes and activating insulin signaling pathway. However, whether FAIM was involved in other pathways of hepatic lipid metabolism, such as fatty acid β-oxidation, remains to be investigated.

Hepatocyte energy homeostasis are maintained by modulators such as AMP-activated protein kinase (AMPK) pathway. AMPK activation eliminates energy surpluses, enhances energy expenditure, and maintains energy homeostasis in response to physiological and nutritional stimulus [50]. AMPK is a key regulatory element of metabolism and has been recognized as a therapeutic target for the treating multiple metabolic disorders [51]. Under energy stress, AMPK signaling pathway was activated to stimulate ATP production, such as fatty acid β-oxidation, and inhibits ATP-consuming pathways, such as lipogenesis. However, chronic HFD exposure reduces AMPK activity and triggers a vicious imbalance of lipogenesis and lipid oxidation, resulting in hepatic lipid accumulation and insulin resistance [51–55]. AMPK activation effectively protects mice against diet-induced hepatic lipid accumulation by inhibiting SREBPs signaling pathway [51]. In this context, we demonstrated that the level of phosphorylated-AMPK increases in FAIM overexpressed mice fed with HFD, but decreases in FAIM knockdown mice fed with HFD. Our study showed that AMPK was a downstream effector of FAIM. However, the detailed signaling mechanism of AMPK

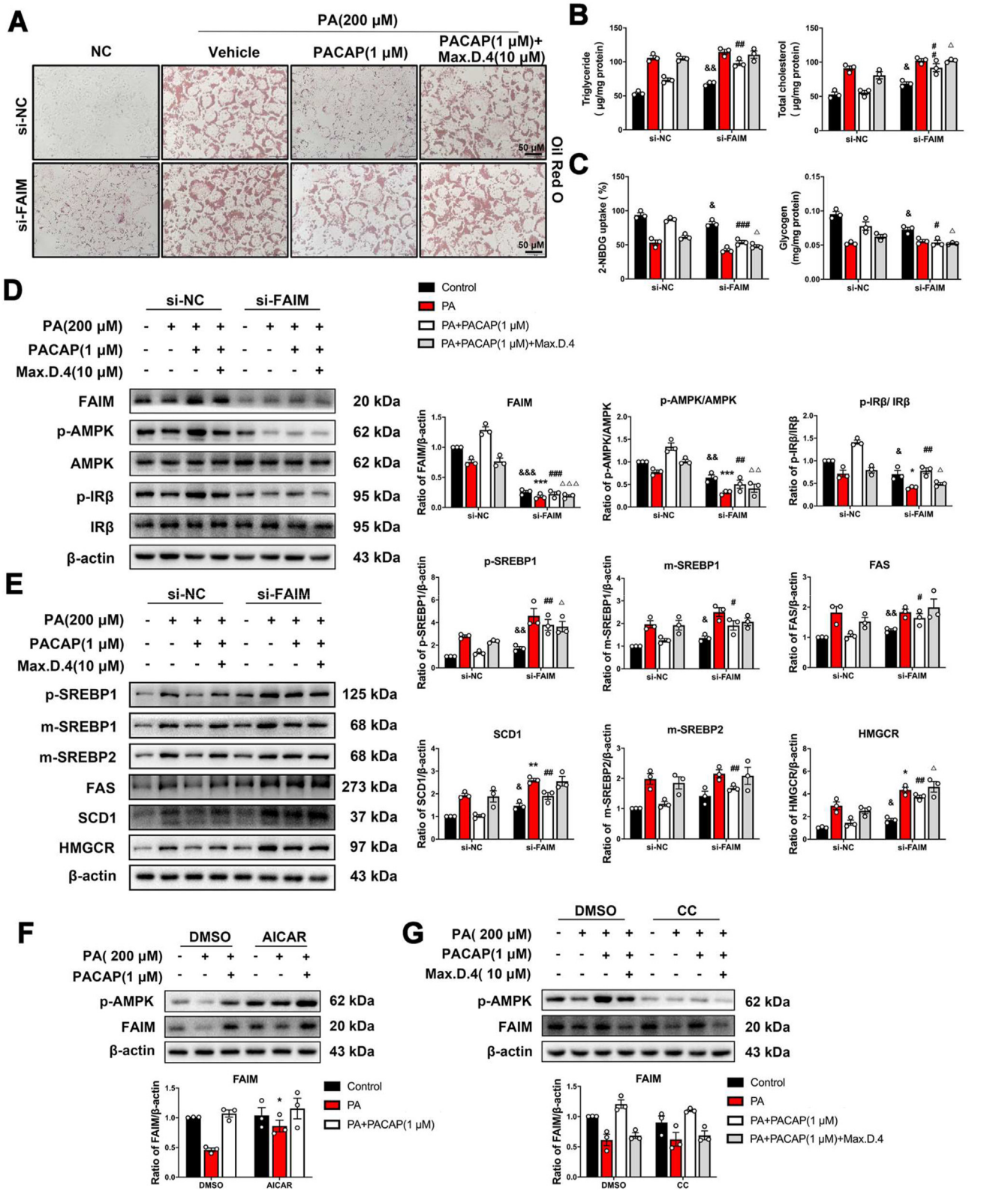

Figure 6: Knockdown of *Faim* inhibited the effects of PACAP on decreasing lipid accumulation and activating AMPK-IRβ signaling pathway. AML12 cells were transiently transfected with *Faim* siRNA or scramble siRNA in cell culture medium containing 200 μM PA or 10% BSA (as control of PA solution) for 24 h, then the cells were treated with PACAP (1 μM) and Max.D.4 (10 μM) for another 24 h as indicated. (A) Representative for Oil Red O staining of AML12 (Scale bars, 50 μM). (B and C) Impacts of *Faim* knockdown on cellular TG and TC level (B), glucose uptake and glycogen content (C) of AML12. (D and E) *Faim* knockdown impaired the activation of AMPK-IRβ pathway in AML12 treated with PACAP, the protein levels were analyzed by western blot and quantitative measurements (right). (F and G) AML12 were exposed to PA for 24 h, then treated with PACAP (1 μM), Max.D.4 (10 μM) and Compound C (10 μM) (F) or AICAR (0.5 mM) (G) for another 24 h. The protein level of FAIM was detected by western blot analysis and quantitative measurements (down). Data are presented as mean ± SEM. n = 3 (&$P < 0.05$, &&$P < 0.01$, &&&$P < 0.001$ *vs.* control group; *$P < 0.05$, **$P < 0.01$, ***$P < 0.001$ *vs.* PA group; #$P < 0.05$, ##$P < 0.01$, ###$P < 0.001$ *vs.* PA + PACAP group, △$P < 0.05$, △△$P < 0.01$, △△△$P < 0.001$ *vs.* PA + PACAP + Max.D.4 group).

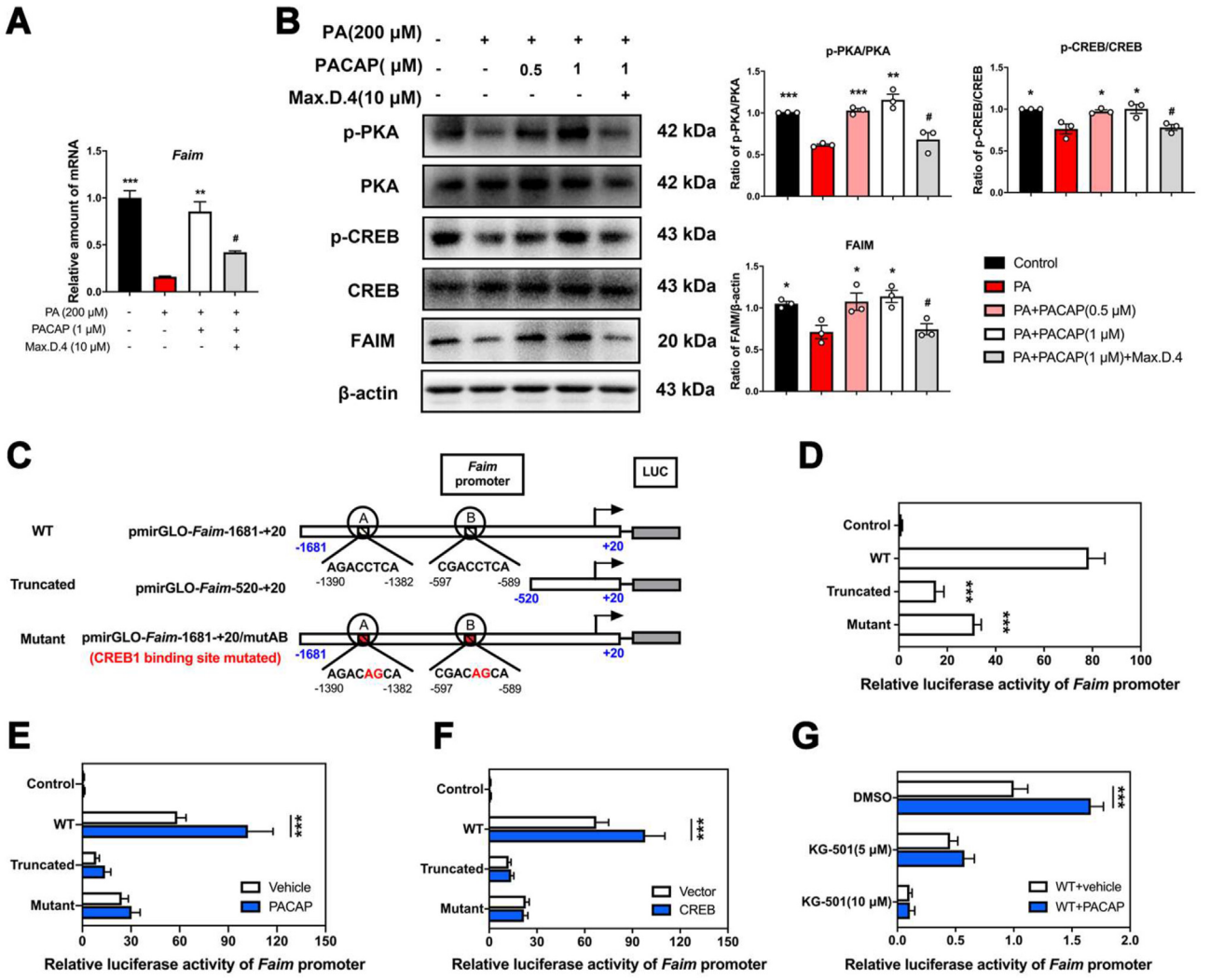

Figure 7: PACAP activates the PAC1-PKA-CREB signaling pathway to stimulate FAIM expression. (A) mRNA level of *Faim* in PA-induced AML12 treated with PACAP, determined by qRT-PCR (n = 3). (B) The effect of PACAP on the activation of PKA and CREB in PA induced AML12 cells, the protein levels of PKA, CREB and FAIM, and phosphorylation of PKA and CREB were determined by western blot. ($^{*}P < 0.05$, $^{**}P < 0.01$, $^{***}P < 0.001$ *vs.* PA group; $\#P < 0.05$, $\#\#P < 0.01$, $\#\#\#P < 0.001$ *vs.* PACAP (1 μM) group). (C) Schematic of the sequence of two CRE binding sites that CREB targets the WT or mutated promoter region of *Faim* mRNA. (D–F) Luciferase activities in AML12 transiently transfected with either wild type (WT), truncated, or mutant *Faim* promoter-luciferase reporter constructs. Then the cells were treated with PACAP (1 μM), or co-transfected with CREB cDNA or empty vectors. (G) Luciferase activities of FAIM WT reporter plasmids in AML12 cells with the treatment of KG-501 (a specific CREB inhibitor) and PACAP (1 μM) as indicated. Data are shown as mean ± SEM, n = 3 or 5 ($^{*}P < 0.05$, $^{**}P < 0.01$, $^{***}P < 0.001$).

activation remains not fully understood. Then, we demonstrated that hepatic FAIM expression was required for the beneficial effect of PACAP in HFD mice. Furthermore, we performed a dual luciferase reporter assay to investigate the effect of PACAP on the *Faim* promoter. The results showed that PACAP promoted the expression of *Faim* transcription level through the PKA-CREB signaling pathway. Based on the results, we propose our hypothesis, that PACAP activates FAIM in the liver, which promotes AMPK and IRβ phosphorylation, thus inhibits lipogenesis to alleviate overnutrition induced hepatic lipid accumulation and insulin resistance. Together, we establish a novel signaling axis that PACAP improves hepatic lipid metabolism through activating AMPK-IRβ in a FAIM-dependent manner.

In summary, our work revealed that PACAP suppressed hepatic lipogenesis and improved insulin sensitivity in overnutrition-induced fatty liver progression through the activation of the FAIM-AMPK-IRβ axis. Dysregulation of this axis results in metabolic disorders such as aberrant hepatic lipid accumulation. The study on the PACAP signaling axis established the important role of PACAP in regulating lipid metabolism, and further implicates that PACAP could serve as a promising therapeutic strategy for the treatment of MAFLD.

AUTHOR CONTRIBUTIONS

YM is the guarantor of this work and takes responsibility for the integrity of the data and the accuracy of the data analysis. WL and YM conceived and designed the study. WL, ZZ, PX performed cellular experiments. WL, JD, YH performed animal experiments. WL and YM analyzed the data and wrote the manuscript.

DATA AVAILABILITY

Data will be made available on request.

ACKNOWLEDGMENTS

This study was supported by the National Natural Science Foundation of China (No. 82073748 and 81741130); Guangdong Basic and Applied Basic Research Foundation (No. 2019A1515011866 and 2021A1515010993); Guangdong Science and Technology Innovation Strategy Special Fund (International Science and Technology cooperation projects, No. 2021A0505030034).

CONFLICT OF INTEREST

The authors declare that there is no conflict of interests.

APPENDIX A. SUPPLEMENTARY DATA

Supplementary data to this article can be found online at https://doi.org/10.1016/j.molmet.2022.101584.

REFERENCES

[1] Samuel, V.T., Shulman, G.I., 2018. Nonalcoholic fatty liver disease as a nexus of metabolic and hepatic diseases. Cell Metabolism 27(1):22—41.

[2] Younossi, Z.M., 2019. Non-alcoholic fatty liver disease - a global public health perspective. Journal of Hepatology 70(3):531—544.

[3] Rotman, Y., Sanyal, A.J., 2017. Current and upcoming pharmacotherapy for non-alcoholic fatty liver disease. Gut 66(1):180—190.

[4] Estes, C., Anstee, Q.M., Arias-Loste, M.T., Bantel, H., Bellentani, S., Caballeria, J., et al., 2018. Modeling NAFLD disease burden in China, France, Germany, Italy, Japan, Spain, United Kingdom, and United States for the period 2016-2030. Journal of Hepatology 69(4):896—904.

[5] Lambert, J.E., Ramos-Roman, M.A., Browning, J.D., Parks, E.J., 2014. Increased de novo lipogenesis is a distinct characteristic of individuals with nonalcoholic fatty liver disease. Gastroenterology 146(3):726—735.

[6] Fabbrini, E., Tiemann Luecking, C., Love-Gregory, L., Okunade, A.L., Yoshino, M., Fraterrigo, G., et al., 2016. Physiological mechanisms of weight gain-induced steatosis in people with obesity. Gastroenterology 150(1):79—81 e2.

[7] Donnelly, K.L., Smith, C.I., Schwarzenberg, S.J., Jessurun, J., Boldt, M.D., Parks, E.J., 2005. Sources of fatty acids stored in liver and secreted via lipoproteins in patients with nonalcoholic fatty liver disease. Journal of Clinical Investigation 115(5):1343—1351.

[8] Bozadjieva-Kramer, N., Ross, R.A., Johnson, D.Q., Fenselau, H., Haggerty, D.L., Atwood, B., et al., 2021. The role of mediobasal hypothalamic PACAP in the control of body weight and metabolism. Endocrinology 162(4).

[9] Rudecki, A.P., Gray, S.L., 2016. PACAP in the defense of energy homeostasis. Trends in Endocrinology and Metabolism 27(9):620—632.

[10] Gray, S.L., Cummings, K.J., Jirik, F.R., Sherwood, N.M., 2001. Targeted disruption of the pituitary adenylate cyclase-activating polypeptide gene results in early postnatal death associated with dysfunction of lipid and carbohydrate metabolism. Molecular Endocrinology 15(10):1739—1747.

[11] Diané, A., Nikolic, N., Rudecki, A.P., King, S.M., Bowie, D.J., Gray, S.L., 2014. PACAP is essential for the adaptive thermogenic response of brown adipose tissue to cold exposure. Journal of Endocrinology 222(3):327—339.

[12] Chang, R., Hernandez, J., Gastelum, C., Guadagno, K., Perez, L., Wagner, E.J., 2021. Pituitary adenylate cyclase-activating polypeptide excites proopiomelanocortin neurons: implications for the regulation of energy homeostasis. Neuroendocrinology 111(1—2):45—69.

[13] Resch, J.M., Maunze, B., Gerhardt, A.K., Magnuson, S.K., Phillips, K.A., Choi, S., 2013. Intrahypothalamic pituitary adenylate cyclase-activating polypeptide regulates energy balance via site-specific actions on feeding and metabolism. American Journal of Physiology. Endocrinology and Metabolism 305(12):E1452—E1463.

[14] Liu, M., Yang, X., Bai, T., Liu, Z., Liu, T., Wang, Y., et al., 2019. PACAP stimulates insulin secretion by PAC(1) receptor and ion channels in β-cells. Cellular Signalling 61:48—56.

[15] Hurley, M.M., Anderson, E.M., Chen, C., Maunze, B., Hess, E.M., Block, M.E., et al., 2020. Acute blockade of PACAP-dependent activity in the ventromedial nucleus of the hypothalamus disrupts leptin-induced behavioral and molecular changes in rats. Neuroendocrinology 110(3—4):271—281.

[16] Xiao, X., Qiu, P., Gong, H.Z., Chen, X.M., Sun, Y., Hong, A., et al., 2019. PACAP ameliorates hepatic metabolism and inflammation through up-regulating FAIM in obesity. Journal of Cellular and Molecular Medicine 23(9):5970—5980.

[17] Schneider, T.J., Fischer, G.M., Donohoe, T.J., Colarusso, T.P., Rothstein, T.L., 1999. A novel gene coding for a Fas apoptosis inhibitory molecule (FAIM) isolated from inducibly Fas-resistant B lymphocytes. Journal of Experimental Medicine 189(6):949—956.

[18] Huo, J., Xu, S., Lam, K.P., 2019. FAIM: an antagonist of fas-killing and beyond. Cells 8(6).

[19] Kaku, H., Rothstein, T.L., 2020. FAIM is a non-redundant defender of cellular viability in the face of heat and oxidative stress and interferes with accumulation of stress-induced protein aggregates. Frontiers in Molecular Biosciences 7:32.

[20] Han, T., Wang, P., Wang, Y., Xun, W., Lei, J., Wang, T., et al., 2021. FAIM regulates autophagy through glutaminolysis in lung adenocarcinoma. Autophagy, 1—17.

[21] Huo, J., Ma, Y., Liu, J.J., Ho, Y.S., Liu, S., Soh, L.Y., et al., 2016. Loss of Fas apoptosis inhibitory molecule leads to spontaneous obesity and hepatosteatosis. Cell Death & Disease 7(2):e2091.

[22] Charni-Natan, M., Goldstein, I., 2020. Protocol for primary mouse hepatocyte isolation. STAR Protocols 1(2):100086.

[23] Cabrera-Cruz, H., Oróstica, L., Plaza-Parrochia, F., Torres-Pinto, I., Romero, C., Vega, M., 2020. The insulin-sensitizing mechanism of myo-inositol is associated with AMPK activation and GLUT-4 expression in human endometrial cells exposed to a PCOS environment. American Journal of Physiology. Endocrinology and Metabolism 318(2):E237-e48.

[24] Yan, Q., Huang, H., Lu, S., Ou, B., Feng, J., Shan, W., et al., 2020. PACAP ameliorates fertility in obese male mice via PKA/CREB pathway-dependent Sirt1 activation and p53 deacetylation. Journal of Cellular Physiology 235(10):7465—7483.

[25] Abid, H., Cartier, D., Hamieh, A., François-Bellan, A.M., Bucharles, C., Pothion, H., et al., 2019. AMPK activation of PGC-1α/NRF-1-dependent SELENOT gene transcription promotes PACAP-induced neuroendocrine cell differentiation through tolerance to oxidative stress. Molecular Neurobiology 56(6):4086—4101.

[26] Thomas-Chollier, M., Hufton, A., Heinig, M., O'Keeffe, S., Masri, N.E., Roider, H.G., et al., 2011. Transcription factor binding predictions using TRAP for the analysis of ChIP-seq data and regulatory SNPs. Nature Protocols 6(12):1860—1869.

[27] Fornes, O., Castro-Mondragon, J.A., Khan, A., van der Lee, R., Zhang, X., Richmond, P.A., et al., 2020. Jaspar 2020: update of the open-access database of transcription factor binding profiles. Nucleic Acids Research 48(D1):D87—D92.

[28] Min, H.K., Kapoor, A., Fuchs, M., Mirshahi, F., Zhou, H., Maher, J., et al., 2012. Increased hepatic synthesis and dysregulation of cholesterol metabolism is associated with the severity of nonalcoholic fatty liver disease. Cell Metabolism 15(5):665—674.

[29] Akesson, L., Ahrén, B., Manganiello, V.C., Holst, L.S., Edgren, G., Degerman, E., 2003. Dual effects of pituitary adenylate cyclase-activating polypeptide and isoproterenol on lipid metabolism and signaling in primary rat adipocytes. Endocrinology 144(12):5293—5299.

[30] Rasbach, E., Splitthoff, P., Bonaterra, G.A., Schwarz, A., Mey, L., Schwarzbach, H., et al., 2019. PACAP deficiency aggravates atherosclerosis in ApoE deficient mice. Immunobiology 224(1):124–132.

[31] Nakata, M., Shintani, N., Hashimoto, H., Baba, A., Yada, T., 2010. Intra-islet PACAP protects pancreatic β-cells against glucotoxicity and lipotoxicity. Journal of Molecular Neuroscience 42(3):404–410.

[32] Yada, T., Sakurada, M., Filipsson, K., Kikuchi, M., Ahrén, B., 2000. Intraperitoneal PACAP administration decreases blood glucose in GK rats, and in normal and high fat diet mice. Annals of the New York Academy of Sciences 921:259–263.

[33] Vuppalanchi, R., Noureddin, M., Alkhouri, N., Sanyal, A.J., 2021. Therapeutic pipeline in nonalcoholic steatohepatitis. Nature Reviews Gastroenterology & Hepatology 18(6):373–392.

[34] Baggio, L.L., Drucker, D.J., 2021. Glucagon-like peptide-1 receptor co-agonists for treating metabolic disease. Molecular Metabolism 46:101090.

[35] Newsome, P.N., Buchholtz, K., Cusi, K., Linder, M., Okanoue, T., Ratziu, V., et al., 2021. A placebo-controlled trial of subcutaneous semaglutide in nonalcoholic steatohepatitis. New England Journal of Medicine 384(12): 1113–1124.

[36] Capehorn, M.S., Catarig, A.M., Furberg, J.K., Janez, A., Price, H.C., Tadayon, S., et al., 2020. Efficacy and safety of once-weekly semaglutide 1.0mg vs once-daily liraglutide 1.2mg as add-on to 1-3 oral antidiabetic drugs in subjects with type 2 diabetes (SUSTAIN 10). Diabetes & Metabolism 46(2): 100–109.

[37] Marso, S.P., Bain, S.C., Consoli, A., Eliaschewitz, F.G., Jódar, E., Leiter, L.A., et al., 2016. Semaglutide and cardiovascular outcomes in patients with type 2 diabetes. New England Journal of Medicine 375(19):1834–1844.

[38] Palmer, S.C., Tendal, B., Mustafa, R.A., Vandvik, P.O., Li, S., Hao, Q., et al., 2021. Sodium-glucose cotransporter protein-2 (SGLT-2) inhibitors and glucagon-like peptide-1 (GLP-1) receptor agonists for type 2 diabetes: systematic review and network meta-analysis of randomised controlled trials. BMJ 372:m4573.

[39] Rosenstock, J., Wysham, C., Frías, J.P., Kaneko, S., Lee, C.J., Fernández Landó, L., et al., 2021. Efficacy and safety of a novel dual GIP and GLP-1 receptor agonist tirzepatide in patients with type 2 diabetes (SURPASS-1): a double-blind, randomised, phase 3 trial. Lancet 398(10295):143–155.

[40] Karpiesiuk, A., Palus, K., 2021. Pituitary adenylate cyclase-activating polypeptide (PACAP) in physiological and pathological processes within the gastrointestinal tract: a review. International Journal of Molecular Sciences 22(16):8682.

[41] Tsutsumi, M., Claus, T.H., Liang, Y., Li, Y., Yang, L., Zhu, J., et al., 2002. A potent and highly selective VPAC2 agonist enhances glucose-induced insulin release and glucose disposal: a potential therapy for type 2 diabetes. Diabetes 51(5):1453–1460.

[42] Ramos-Álvarez, I., Mantey, S.A., Nakamura, T., Nuche-Berenguer, B., Moreno, P., Moody, T.W., et al., 2015. A structure-function study of PACAP using conformationally restricted analogs: identification of PAC1 receptor-selective PACAP agonists. Peptides 66:26–42.

[43] Bourgault, S., Vaudry, D., Botia, B., Couvineau, A., Laburthe, M., Vaudry, H., et al., 2008. Novel stable PACAP analogs with potent activity towards the PAC1 receptor. Peptides 29(6):919–932.

[44] Ma, Y., Fang, S., Zhao, S., Wang, X., Wang, D., Ma, M., et al., 2015. A recombinant slow-release PACAP-derived peptide alleviates diabetes by promoting both insulin secretion and actions. Biomaterials 51:80–90.

[45] Zhuang, M., Du, D., Pu, L., Song, H., Deng, M., Long, Q., et al., 2019. SPION-decorated exosome delivered BAY55-9837 targeting the pancreas through magnetism to improve the blood GLC response. Small 15(52):e1903135.

[46] Coccia, E., Masanas, M., López-Soriano, J., Segura, M.F., Comella, J.X., Pérez-García, M.J., 2020. FAIM is regulated by MiR-206, MiR-1-3p and MiR-133b. Frontiers in Cell and Developmental Biology 8:584606.

[47] Wang, P., Xun, W., Han, T., Cheng, Z., 2020. FAIM-S functions as a negative regulator of NF-κB pathway and blocks cell cycle progression in NSCLC cells. Cell Cycle 19(24):3458–3467.

[48] Sole, C., Dolcet, X., Segura, M.F., Gutierrez, H., Diaz-Meco, M.T., Gozzelino, R., et al., 2004. The death receptor antagonist FAIM promotes neurite outgrowth by a mechanism that depends on ERK and NF-kapp B signaling. The Journal of Cell Biology 167(3):479–492.

[49] Kaku, H., Rothstein, T.L., 2009. Fas apoptosis inhibitory molecule enhances CD40 signaling in B cells and augments the plasma cell compartment. Journal of Immunology 183(3):1667–1674.

[50] Herzig, S., Shaw, R.J., 2018. AMPK: guardian of metabolism and mitochondrial homeostasis. Nature Reviews Molecular Cell Biology 19(2):121–135.

[51] Mottillo, E.P., Desjardins, E.M., Crane, J.D., Smith, B.K., Green, A.E., Ducommun, S., et al., 2016. Lack of adipocyte AMPK exacerbates insulin resistance and hepatic steatosis through Brown and beige adipose tissue function. Cell Metabolism 24(1):118–129.

[52] Li, S., Qian, Q., Ying, N., Lai, J., Feng, L., Zheng, S., et al., 2020. Activation of the AMPK-SIRT1 pathway contributes to protective effects of Salvianolic acid A against lipotoxicity in hepatocytes and NAFLD in mice. Frontiers in Pharmacology 11:560905.

[53] Smith, B.K., Marcinko, K., Desjardins, E.M., Lally, J.S., Ford, R.J., Steinberg, G.R., 2016. Treatment of nonalcoholic fatty liver disease: role of AMPK. American Journal of Physiology. Endocrinology and Metabolism 311(4): E730-e40.

[54] Lindholm, C.R., Ertel, R.L., Bauwens, J.D., Schmuck, E.G., Mulligan, J.D., Saupe, K.W., 2013. A high-fat diet decreases AMPK activity in multiple tissues in the absence of hyperglycemia or systemic inflammation in rats. Journal of Physiology & Biochemistry 69(2):165–175.

[55] Huang, H., Lee, S.H., Sousa-Lima, I., Kim, S.S., Hwang, W.M., Dagon, Y., et al., 2018. Rho-kinase/AMPK axis regulates hepatic lipogenesis during overnutrition. Journal of Clinical Investigation 128(12):5335–5350.

